

Ground-state properties of trapped Bose-Fermi mixtures: Role of exchange correlation

Alexander P. Albus,¹ Fabrizio Illuminati,² and Martin Wilkens¹¹*Institut für Physik, Universität Potsdam, D-14469 Potsdam, Germany*²*Dipartimento di Fisica, Università di Salerno, and Istituto Nazionale per la Fisica della Materia, I-84081 Baronissi (SA), Italy*

(Received 10 February 2003; published 19 June 2003)

We introduce density-functional theory for inhomogeneous Bose-Fermi mixtures, derive the associated Kohn-Sham equations, and determine the exchange-correlation energy in local-density approximation. We solve numerically the Kohn-Sham system, and determine the boson and fermion density distributions and the ground-state energy of a trapped, dilute mixture beyond mean-field approximation. The importance of the corrections due to exchange correlation is discussed by a comparison with current experiments; in particular, we investigate the effect of the repulsive potential-energy contribution due to exchange correlation on the stability of the mixture against collapse.

DOI: 10.1103/PhysRevA.67.063606

PACS number(s): 03.75.Mn, 71.15.Mb

I. INTRODUCTION

The achievement of Bose-Einstein condensation in trapped, dilute alkali-metal gases [1] has stimulated a rapidly growing activity in the field of ultracold, degenerate quantum gases, aimed at a better understanding of fundamental aspects of the quantum theory. In particular, recent experimental progresses have opened the way to the fascinating prospect of realizing a BCS transition to superfluidity in ultracold, trapped Fermi gases.

Magnetically trapped fermions interact very weakly, as their spins are polarized in the direction of the trapping magnetic field, so that fermion-fermion s -wave scattering is prevented by the Pauli principle. Cooling of the fermions to quantum degeneracy can then be efficiently achieved by mixing them with ultracold bosons. After the process of sympathetic cooling, the final phase of the system is a quantum degenerate Bose-Fermi mixture. Indeed, such a system has been recently realized experimentally [2–5].

On the theoretical side, dilute Bose-Fermi mixtures have been studied in both homogeneous and confined geometries. For homogeneous systems, recent work has addressed the problem of stability and phase separation [6]; the effect of boson-fermion interactions on the dynamics [7]; and the BCS transition induced on the fermions by the boson-fermion interactions [8]. The first correction to the ground-state energy beyond the mean-field approximation has been determined analytically for homogeneous systems [9]. This exchange-correlation term can be used for trapped systems in the local-density approximation, i.e., when the interaction length scales are much smaller than the characteristic sizes of the trapping potentials. This condition is naturally met in the current experiments. Recent numerical work [10] confirms the analytical findings in the corresponding regime for homogeneous systems.

For trapped systems, the theory has been developed in the mean-field approximation to determine the boson and fermion density profiles at zero temperature [11], and the related properties of stability against phase separation and collapse [12]. A mean-field approach has been also employed to calculate the critical temperature of Bose-Einstein condensation in a trapped mixture [13]. However, a description be-

yond mean field is needed either when the interaction parameters are large, or to gain a very precise knowledge of the density profiles and the related properties of stability. In the present work, we determine the ground-state energy and the boson and fermion density profiles to second order in the boson-fermion scattering length for harmonically trapped Bose-Fermi mixtures at zero temperature, and determine the modification, due to the resulting exchange-correlation energy, of the mean-field predictions.

The plan of the paper is the following. In Sec. II, we briefly show how to apply density-functional theory (DFT) [14] to inhomogeneous boson-fermion systems, and we determine the exchange-correlation energy functional via local-density approximation (LDA) on the ground-state energy functional of homogeneous mixtures beyond mean field obtained in Ref. [9]. In Sec. III, we provide the numerical solution of the coupled, nonlinear Kohn-Sham equations for the boson and fermion density distributions, and we determine the importance of the corrections due to exchange correlation by comparing our results with current experiments. In Sec. IV, we discuss the effect of the exchange-correlation energy term on the phase diagram of the mixture, especially regarding the onset of collapse for mixtures with attractive boson-fermion interaction.

II. THEORY

We begin by considering an inhomogeneous, dilute system of interacting bosons and spin-polarized fermions with two-body interactions in the s -wave scattering approximation, so that the interparticle potentials are $U_{BB}(|\mathbf{r}-\mathbf{r}'|) = g_{BB}\delta(\mathbf{r}-\mathbf{r}')$, $U_{FF}(|\mathbf{r}-\mathbf{r}'|) = 0$, and $U_{BF}(|\mathbf{r}-\mathbf{r}'|) = g_{BF}\delta(\mathbf{r}-\mathbf{r}')$. The boson-boson coupling is $g_{BB} = 4\pi\hbar^2 a_{BB}/m_B$, where a_{BB} is the boson-boson s -wave scattering length and m_B is the boson mass. The boson-fermion coupling reads $g_{BF} = 2\pi\hbar^2 a_{BF}/m_R$, where a_{BF} is the boson-fermion s -wave scattering length and $m_R = m_B m_F / (m_B + m_F)$ is the reduced mass (m_F is the fermion mass). The full Hamiltonian reads

$$\hat{H} = \hat{T}_B + \hat{T}_F + \hat{V}_B + \hat{V}_F + \hat{W}_{BB} + \hat{W}_{BF}, \quad (1)$$

where

$$\begin{aligned}\hat{T}_B &= - \int d\mathbf{r} \hat{\Phi}^\dagger(\mathbf{r}) \frac{\hbar^2 \nabla^2}{2m_B} \hat{\Phi}(\mathbf{r}); & \hat{V}_B &= \int d\mathbf{r} \hat{\Phi}^\dagger(\mathbf{r}) V_B \hat{\Phi}(\mathbf{r}), \\ \hat{T}_F &= - \int d\mathbf{r} \hat{\Psi}^\dagger(\mathbf{r}) \frac{\hbar^2 \nabla^2}{2m_F} \hat{\Psi}(\mathbf{r}); & \hat{V}_F &= \int d\mathbf{r} \hat{\Psi}^\dagger(\mathbf{r}) V_F \hat{\Psi}(\mathbf{r}), \\ \hat{W}_{BB} &= \frac{1}{2} \int \int d\mathbf{r} d\mathbf{r}' \hat{\Phi}^\dagger(\mathbf{r}) \hat{\Phi}^\dagger(\mathbf{r}') U_{BB} \hat{\Phi}(\mathbf{r}') \hat{\Phi}(\mathbf{r}), \\ \hat{W}_{BF} &= \int \int d\mathbf{r} d\mathbf{r}' \hat{\Phi}^\dagger(\mathbf{r}) \hat{\Psi}^\dagger(\mathbf{r}') U_{BF} \hat{\Psi}(\mathbf{r}') \hat{\Phi}(\mathbf{r}).\end{aligned}\quad (2)$$

Here, \hat{T}_B and \hat{T}_F denote the boson and fermion kinetic energies, $V_B(\mathbf{r})$ and $V_F(\mathbf{r})$ denote the boson and fermion trapping potentials, and $\hat{\Phi}(\mathbf{r})$ and $\hat{\Psi}(\mathbf{r})$ represent the boson and fermion field operators.

Let the ground state of the system be $|g\rangle$, and introduce the ground-state energy $E_0 \stackrel{\text{def}}{=} \langle g | \hat{H} | g \rangle$, and the boson and fermion densities $n_B(\mathbf{r}) \stackrel{\text{def}}{=} \langle g | \hat{\Phi}^\dagger(\mathbf{r}) \hat{\Phi}(\mathbf{r}) | g \rangle$ and $n_F(\mathbf{r}) \stackrel{\text{def}}{=} \langle g | \hat{\Psi}^\dagger(\mathbf{r}) \hat{\Psi}(\mathbf{r}) | g \rangle$. The Hohenberg-Kohn theorem [14] guarantees that, given the interaction potentials, the ground-state energy depends only on the densities, i.e., it is a functional $E_0 = E_0[n_B, n_F]$. The theorem was proved originally for Fermi systems, but its generalization to Bose systems and to Bose-Fermi mixtures is straightforward. Determination of the density distributions follows by imposing the stationarity conditions

$$\frac{\delta E_0[n_B, n_F]}{\delta n_B(\mathbf{r})} \stackrel{!}{=} \mu_B; \quad \frac{\delta E_0[n_B, n_F]}{\delta n_F(\mathbf{r})} \stackrel{!}{=} \mu_F, \quad (3)$$

where μ_B and μ_F are the boson and fermion chemical potentials, respectively.

In general, the functional $E_0[n_B, n_F]$ cannot be determined exactly, but we can follow the Kohn-Sham procedure [14] to introduce accurate approximations. The idea is to map the interacting systems of interest to a noninteracting reference system with the same density distributions:

$n_B(\mathbf{r}) \mapsto n_B^{\text{ref}}(\mathbf{r}) = n_B(\mathbf{r}); n_F(\mathbf{r}) \mapsto n_F^{\text{ref}}(\mathbf{r}) = n_F(\mathbf{r})$. Uniqueness of the mapping follows from the Hohenberg-Kohn theorem, and we find

$$\begin{aligned}E_0 &= T_B^{\text{ref}}[n_B, n_F] + T_F^{\text{ref}}[n_B, n_F] + \int d\mathbf{r} V_B n_B + \int d\mathbf{r} V_F n_F \\ &+ \frac{g_{BB}}{2} \int d\mathbf{r} n_B^2 + g_{BF} \int d\mathbf{r} n_B n_F + E_{\text{xc}}[n_B, n_F],\end{aligned}\quad (4)$$

where the first two terms are the kinetic energies of the reference system, the next two terms are the trapping energies, and the fifth and sixth terms are the mean-field part of the interaction energy. The last term includes all the contributions to the interaction energy beyond mean field due to exchange correlations, and defines the exchange-correlation energy functional $E_{\text{xc}}[n_B, n_F]$. If E_{xc} is neglected altogether, one simply recovers the equations of mean-field theory for trapped Bose-Fermi mixtures [11,12].

We now proceed to carry out the full Kohn-Sham scheme to determine the ground-state energy, and the boson and fermion density profiles beyond mean field. In the Kohn-Sham reference system, the kinetic parts of the energy functional $T_B^{\text{ref}}[n_B, n_F]$ for the bosons and $T_F^{\text{ref}}[n_B, n_F]$ for the fermions are defined as

$$\begin{aligned}T_B^{\text{ref}}[n_B, n_F] &= -N_B \int d^3\mathbf{r} \phi^*(\mathbf{r}) \frac{\hbar^2 \nabla^2}{2m_B} \phi(\mathbf{r}), \\ T_F^{\text{ref}}[n_B, n_F] &= - \sum_{i=1}^{N_F} \int d^3\mathbf{r} \psi_i^*(\mathbf{r}) \frac{\hbar^2 \nabla^2}{2m_F} \psi_i(\mathbf{r}),\end{aligned}\quad (5)$$

where N_B and N_F are the total numbers of bosons and fermions, and the notations $\phi(\mathbf{r})$ and $\psi_i(\mathbf{r})$ are shorthand for the boson and fermion functional orbitals $\phi[n_B, n_F](\mathbf{r})$ and $\psi_i[n_B, n_F](\mathbf{r})$ of the noninteracting reference system, respectively. Substituting Eqs. (5) into Eq. (4) and carrying out the functional derivatives in Eqs. (3), we obtain a system of coupled, effective Schrödinger equations for the single-particle states that are the desired Kohn-Sham equations for a Bose-Fermi system:

$$\begin{aligned}\left[-\frac{\hbar^2 \nabla^2}{2m_B} + V_B + \frac{4\pi\hbar^2 a_{BB}}{m_B} n_B + \frac{2\pi\hbar^2 a_{BF}}{m_R} n_F + \frac{\delta E_{\text{xc}}}{\delta n_B} \right] \phi \\ = \mu_B \phi, \\ \left[-\frac{\hbar^2 \nabla^2}{2m_F} + V_F + \frac{2\pi\hbar^2 a_{BF}}{m_R} n_B + \frac{\delta E_{\text{xc}}}{\delta n_F} \right] \psi_i = \epsilon_i \psi_i,\end{aligned}\quad (6)$$

with $n_B(\mathbf{r}) = N_B |\phi(\mathbf{r})|^2$, $n_F(\mathbf{r}) = \sum_{i=1}^{N_F} |\psi_i(\mathbf{r})|^2$, where the sum in $n_F(\mathbf{r})$ runs over the N_F single-particle states ψ_i with lowest energies ϵ_i . We now resort to LDA by approximating E_{xc} with an integral over the exchange-correlation energy density $E_{\text{xc}}^{\text{hom}}(n_B(\mathbf{r}), n_F(\mathbf{r}))$ of a homogeneous system taken at the—yet unknown—densities $n_B(\mathbf{r})$ and $n_F(\mathbf{r})$:

$$E_{\text{xc}}[n_B, n_F] \approx \int d\mathbf{r} E_{\text{xc}}^{\text{hom}}(n_B, n_F). \quad (7)$$

With this identification, functional derivatives become ordinary partial derivatives:

$$\frac{\delta E_{\text{xc}}}{\delta n_B} = \frac{\partial E_{\text{xc}}^{\text{hom}}}{\partial n_B}; \quad \frac{\delta E_{\text{xc}}}{\delta n_F} = \frac{\partial E_{\text{xc}}^{\text{hom}}}{\partial n_F}. \quad (8)$$

The homogeneous exchange-correlation energy density $E_{\text{xc}}^{\text{hom}}$ has been recently determined [9] to second order in the boson-fermion scattering length a_{BF} via a T -matrix approach analog of the Beliaev expansion for a pure Bose system [15], and its expression reads [9]

$$E_{\text{xc}}^{\text{hom}}(n_B, n_F) = \frac{2\hbar^2 a_{BF}^2}{m_R} f(\delta) k_F n_F n_B, \quad (9)$$

where $k_F = (6\pi^2 n_F)^{1/3}$ is the Fermi wave vector, and $f(\delta)$ is a dimensionless function that depends only on the boson and fermion masses:

$$f(\delta) = 1 - \frac{3 + \delta}{4\delta} + \frac{3(1 + \delta)^2(1 - \delta)}{8\delta^2} \ln \frac{1 + \delta}{1 - \delta}, \quad (10)$$

with $\delta = (m_B - m_F)/(m_B + m_F)$. Viverit and Giorgini have recently shown [10] that Eq. (9) is exact in the limit $k_F \xi_B \gg 1$, where $\xi_B = 1/\sqrt{8\pi n_B a_{BB}}$ is the boson healing length. In order of magnitude, the homogeneous densities are $n_F \approx N_F/\ell^3$ and $n_B \approx N_B/\ell^3$, where ℓ is the characteristic length of the confining potential. The condition $k_F \xi_B \gg 1$ is then equivalent to $N_F \gg N_B^{3/2} (a_{BB}/\ell)^{3/2}$. On the other hand, LDA is correct for large N_B and N_F , provided that $\ell \gg a_{BB}, a_{BF}$, i.e., the characteristic lengths of the confining potentials are much larger than the scattering lengths. In current experiments $N_F \approx N_B \approx 10^4$ and $a_{BF}/\ell \approx a_{BB}/\ell \approx 10^{-3}$, so that the condition $k_F \xi_B \gg 1$ is well satisfied. Moreover, the boson-boson exchange-correlation energy is $256\hbar^2 a_{BB} n_B^2 \sqrt{\pi n_B a_{BB}^3}/15m_B$ (see, e.g., Ref. [15]). This is much smaller than the exchange-correlation energy (9) if $N_F \gg 5.4(a_{BB}/a_{BF})^{3/2} (a_{BB}/\ell)^{3/8} [(1 - \delta)/f(\delta)] N_B^{9/8}$. Since $a_{BB}/a_{BF} = 0.13$ for the Paris experiment with ${}^6\text{Li}$ - ${}^7\text{Li}$ [3] and $a_{BB}/a_{BF} = 0.28$ for the Florence experiment with ${}^{40}\text{K}$ - ${}^{87}\text{Rb}$ [5] (these are the only two experiments where a_{BF} has been measured), this condition is satisfied as well. Yet other higher-order terms are due to direct Fermion-Fermion p -wave scattering. These terms are at least of the order of $(k_F a_{FF})^3$, where a_{FF} is the Fermion-Fermion p -wave scattering length, and thus certainly negligible against the term we consider. Altogether, Eq. (9) provides the most relevant contribution to the exchange-correlation energy for the current experimental situations. For more general situations, Eq. (9) provides the most relevant contribution beyond mean field any time LDA is satisfied, N_F is comparable or larger than N_B in order of magnitude, and perturbation theory holds, i.e., $k_F a_{BF}/\pi \ll 1$, and a sufficiently small Bose gas parameter.

We now consider the Kohn-Sham system (6) with the exchange-correlation energy (9) for spherically symmetric, harmonically trapped systems: $V_B(\mathbf{r}) = (m_B \omega_B^2 r^2)/2$, $V_F(\mathbf{r}) = (m_F \omega_F^2 r^2)/2$. Due to the spherical symmetry, we can write

$$\phi(\mathbf{r}) = \frac{u(r)}{r} Y_{00}; \quad \psi_{nlm}(\mathbf{r}) = \frac{u_{nl}(r)}{r} Y_{lm}, \quad (11)$$

where $Y_{lm}(\Theta, \Phi)$ are the spherical harmonics, and the Kohn-Sham equations (6) become

$$\left[-\frac{1}{2m_B} \frac{d^2}{dr^2} + \frac{m_B}{2} \omega_B^2 r^2 + \frac{4\pi a_{BB}}{m_B} n_B(r) + \frac{2\pi a_{BF}}{m_R} n_F(r) + \frac{2a_{BF}^2 f(\delta)}{m_R} n_F(r) k_F(r) \right] u(r) = \mu_B u(r);$$

$$\left[-\frac{1}{2m_F} \frac{d^2}{dr^2} + \frac{l(l+1)}{2m_F r^2} + \frac{m_F}{2} \omega_F^2 r^2 + \frac{2\pi a_{BF}}{m_R} n_B(r) + \frac{8a_{BF}^2 f(\delta)}{3m_R} n_B(r) k_F(r) \right] u_{nl}(r) = \epsilon_{nl} u_{nl}(r), \quad (12)$$

with $\int dr u^2(r) = 1, \int dr u_{nl}^2(r) = 1$, where n denotes the number of nodes of the radial functions u_{nl} . The normalized density distributions $\tilde{n}_B(\mathbf{r}) = 4\pi r^2 n_B(\mathbf{r})$ and $\tilde{n}_F(\mathbf{r}) = 4\pi r^2 n_F(\mathbf{r})$ are

$$\tilde{n}_B(\mathbf{r}) = N_B u^2(r), \quad (13)$$

and

$$\tilde{n}_F(\mathbf{r}) = \sum_{\epsilon_{nl} \leq \mu_F} (2l+1) u_{nl}^2(r). \quad (14)$$

III. SOLUTION OF THE KOHN-SHAM EQUATIONS

The above expressions together with Eqs. (12) define a system of coupled nonlinear differential equations. The numerical solution is obtained iteratively. We initialize $n_B(\mathbf{r})$ and $n_F(\mathbf{r})$ to be the Thomas-Fermi density distributions with no boson-fermion coupling. We then use these as initial densities for Eqs. (12). The energy eigenvalues are found by a bisection algorithm, iterating the procedure to the desired degree of accuracy. Knowing the states u and u_{nl} , one must determine the wave function u_{nl} with lowest energy ϵ_{nl} using the fact that ϵ_{nl} grows with n and l . When all the occupied Kohn-Sham states are determined, the output densities are compared to the initial distributions. If these are about the same, a self-consistent solution is reached, and the procedure ends. If not, one defines a convex combination of the initial and output densities, $n_{B(F)}^{new}(r) = (1-x)n_{B(F)}^{initial} + x n_{B(F)}^{output}$, with $0 < x \leq 1$, and iterates the procedure until convergence is reached with the desired degree of accuracy. If N_F is large, the procedure is very time consuming and limited by a maximum number of nodes that can be included. One then adopts a Thomas-Fermi approximation for the fermion kinetic energy, whenever $N_F \geq 1000$, and finds a posteriori a very good agreement with the single-particle description.

A comparison of our results with current experiments can be carried out for those systems whose boson-fermion scattering length has been measured. These are the ${}^6\text{Li}$ - ${}^7\text{Li}$ mixtures realized in the Paris experiment [3], and the ${}^{40}\text{K}$ - ${}^{87}\text{Rb}$ recently realized in the Florence experiment [5]. In the Paris experiment with fermionic ${}^6\text{Li}$ and bosonic ${}^7\text{Li}$, the measured scattering lengths are $a_{BB} = 5.1a_0$ and $a_{BF} = 38.0a_0$, where a_0 is the Bohr radius. Taking ω_B as the unit of frequency, the exchange-correlation energy turns out to be $\approx 50\hbar\omega_B$, whereas the mean-field boson-fermion interaction energy is $\approx 7455\hbar\omega_B$. Thus, only about 0.67% of the interaction energy is due to exchange correlations, it has the same sign of the mean-field energy, and the modification of the mean-field density profiles is negligible.

The situation is very different for the mixture of fermionic ${}^{40}\text{K}$ and bosonic ${}^{87}\text{Rb}$ realized in the Florence experiment,

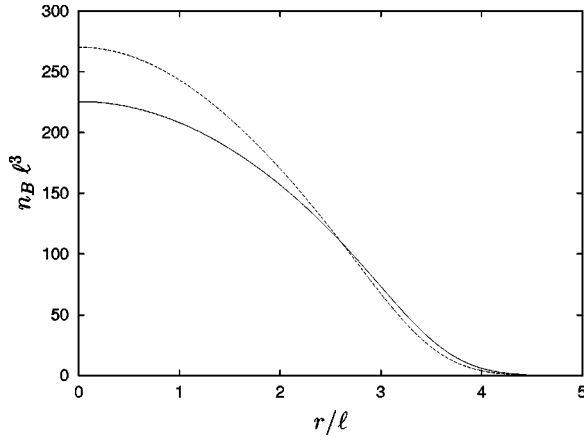


FIG. 1. The boson density profile for the Florence experiment. Dashed line: without exchange correlations; solid line: with exchange correlations. Quantities are dimensionless, rescaled in units of $\ell = (\hbar/m_B\omega_B)^{1/2}$.

due to the large and negative boson-fermion scattering length giving rise both to a large attractive mean-field boson-fermion interaction potential and to a non-negligible exchange-correlation potential. The latter, being proportional to the square of the boson-fermion scattering length, is always repulsive. For this experiment, a typical stable configuration is achieved for $N_F = 10^4$, $N_B = 2 \times 10^4$. The boson-boson scattering length is $a_{BB} = 100a_0$, while the boson-fermion scattering length $a_{BF} \approx -400a_0$ is measured with an uncertainty of about 50%. The mean-field interaction energy is $\approx -98165\hbar\omega_B$, while the exchange-correlation energy is $\approx 6783\hbar\omega_B$. Thus, the relative correction in the interaction energy is about 7% of the mean-field result, going in the opposite direction, and leads to a pronounced effect on the density profiles. Both the boson and fermion densities spread out and decrease substantially at the center of the trap with respect to the mean-field prediction, due to the repulsive exchange-correlation potential. This effect is shown in Figs. 1 and 2, where we show the boson and fermion density dis-

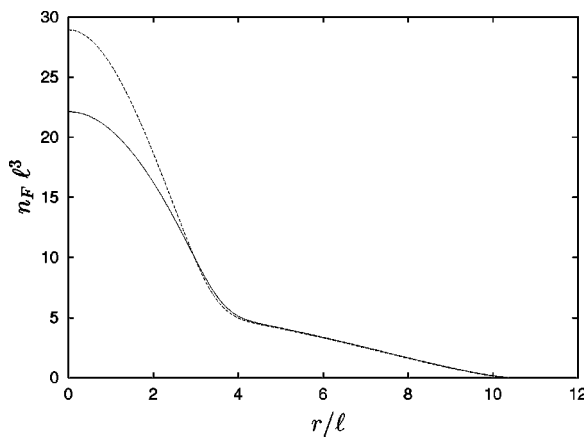


FIG. 2. The fermion density profile for the Florence experiment. Dashed line: without exchange correlations; solid line: with exchange correlations. Quantities are dimensionless, rescaled in units of $\ell = (\hbar/m_B\omega_B)^{1/2}$.

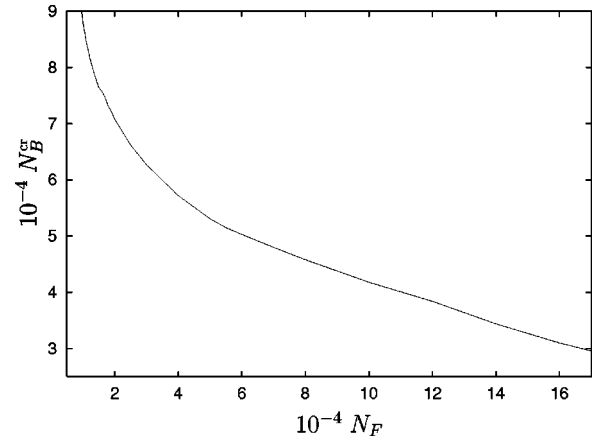


FIG. 3. The critical number of bosons N_B^{cr} for the onset of collapse as a function of the number of fermions N_F in the mean-field approximation.

tributions with and without exchange correlations, calculated with the parameters fixed at the values measured in the Florence experiment. At the center of the trap, the boson and fermion densities are reduced, respectively, to about 85% and 78% of the mean-field result.

IV. STABILITY AND COLLAPSE

In general, there are two kinds of instabilities in a binary mixture (we do not consider instabilities due to fermion pairing): demixing [11] and simultaneous collapse of both the boson and the fermion component [16]. The first can occur if the interaction between the two species is repulsive, and implies by definition a minimal overlap of the density distributions. In this case, we do not expect a significant change of the phase diagram by repulsive exchange-correlation interactions, but only for a small enhancement of the phase separation.

In the collapse regime, which can occur if the interaction between the two species is attractive, the situation is radically different, as in this case one has indeed a very high overlap of the densities in the center of the trap. The exchange-correlation interaction, which is always repulsive to second order in the boson-fermion scattering length, opposes the propensity to collapse due to the attractive mean-field contribution. If the coupling strength between the two components of the mixture is sufficiently strong, the exchange-correlation can significantly modify the phase diagram.

In Fig. 3, we provide the mean-field phase diagram of a binary boson-fermion mixture, with the physical parameters of the Florence experiment [17]. The plot shows the behavior of the critical number of bosons N_B^{cr} , i.e., the threshold number for the onset of collapse, as a function of the number of fermions N_F . Collapse occurs at any point of the phase plane above the critical curve, while the mixture is stable at all points below it. For low fermion numbers $N_F \leq 8 \times 10^3$, the critical number of bosons N_B^{cr} begins to grow so fast that to all practical purposes collapse is inhibited. The inversion regime between the number of fermions and the critical num-

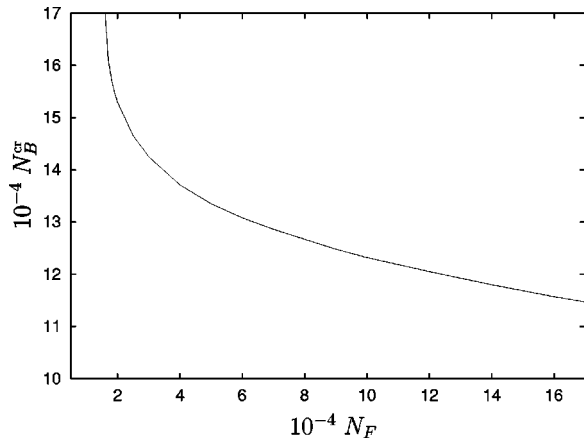


FIG. 4. The critical number of bosons N_B^{cr} for the onset of collapse as a function of the number of fermions N_F including exchange correlation.

ber of bosons takes place at $N_F \approx N_B^{cr} \approx 5 \times 10^4$. For a typical number of fermions $N_F \approx 2 \times 10^4$, one has a critical boson number $N_B^{cr} \approx 7 \times 10^4$. The situation in the mean-field approximation is to be compared with the prediction obtained by including exchange correlation. Figure 4 shows the same phase diagram as in Fig. 3, but with the inclusion of exchange correlation. We clearly see a significant increase in the critical number of the bosons due to exchange correlation. The inversion regime between the number of fermions and the critical number of bosons takes place at $N_F \approx N_B^{cr} \approx 1.2 \times 10^5$, and for a typical fermion number $N_F \approx 2 \times 10^4$ the critical boson number $N_B^{cr} \approx 1.5 \times 10^5$, i.e., a much larger number of bosons is needed to produce a collapse of the fermion component. This behavior was qualitatively expected since the effective exchange-correlation potentials are always repulsive to second order in the boson-fermion scattering length.

The quantitative difference between the mean-field and the exchange-correlation phase diagrams deserves some explanatory comments. First of all, the determination of the critical line for simultaneous collapse takes place in a regime where the numerics is very sensitive to small deviations of the input parameters. Thus, when a stable solution is not found, this could be ascribed either to the fact that the physical collapse regime was reached or to an inappropriate numerical precision. However, by increasing the numerical precision, computation time rapidly increases as well. On the other hand, if a stable numerical solution is found, there can certainly be no physical collapse. The critical curves we present are then lower bounds on the critical numbers. We

remark that the mixture is very sensitive to the exact value of the boson-fermion scattering length in the collapse regime. Since this value is experimentally known with a large uncertainty, it would be crucial to determine it with a much greater precision. This could be achieved by tuning the scattering length in order to fit the experimental data on the onset of collapse [18]. Moreover, for large interaction strengths, such as that in the Florence experiment, the second-order term in the exchange-correlation energy might overestimate the effect of stabilization. In fact, in these cases, the attractive third-order term could possibly give rise to a non-negligible contribution, so that the mean-field critical line of Fig. 3 and the second-order critical line of Fig. 4 would provide, respectively, a lower and an upper bound. The true phase diagram would, therefore, lie in between the two. A more detailed analysis than that provided in the present paper requires, however, analytical expressions of the third-order interaction energy in powers of $k_F a_{BF}$, and this is a formidable task, because Feynman diagrams containing all possible combinations of Boson-Fermion and Boson-Boson interactions have to be considered. These effects cannot be simply determined by resumming restricted classes of equivalent diagrams. Finally, to go beyond second-order perturbation theory requires, for consistency, to take into account interaction processes beyond s -wave scattering, such as p -wave scattering, thus introducing powers of, e.g., the p -wave Boson-Fermion scattering length, and the description soon becomes exceedingly complex in the framework of perturbation theory. Non-perturbative methods, such as Monte Carlo simulations, would then be desirable to establish more accurate results.

In conclusion, we have introduced the Kohn-Sham scheme of DFT for inhomogeneous Bose-Fermi systems to determine the ground-state energy and density profiles to second order in the boson-fermion scattering length. We have compared the theoretical predictions with current experiments, discussed the relevance of different exchange-correlation terms, and investigated the importance of the exchange-correlation effects for dilute atomic gases. We have shown that these are substantial for systems, such as ^{40}K - ^{87}Rb , with a large attractive boson-fermion interaction, especially in the critical regime of collapse onset, by comparing the mean-field phase diagram with the exchange-correlation phase diagram. The DFT method outlined here can be, in principle, extended to include higher-order corrections and finite temperature effects.

We thank H. Hu and M. Modugno for useful comments on an earlier draft of our work, and for stimulating conversations. A.A. and M.W. thank the DFG and the ESF for financial support. F.I. thanks the INFM for financial support.

- [1] W. Ketterle, D.S. Durfee, and D.M. Stamper-Kurn, in *Bose-Einstein Condensation in Atomic Gases*, edited by M. Inguscio, S. Stringari, and C.E. Wieman (SIF, Bologna, 1999), p. 67; E.A. Cornell, J.R. Ensher, and C.E. Wieman, *ibid.*, p. 15.
 [2] A.G. Truscott, K.E. Strecker, W.I. McAlexander, G.B. Partridge, and R.G. Hulet, *Science* **291**, 2570 (2001).

- [3] F. Schreck, L. Khaykovich, K.L. Corwin, G. Ferrari, T. Bourdel, J. Cubizolles, and C. Salomon, *Phys. Rev. Lett.* **87**, 080403 (2001).
 [4] Z. Hadzibabic, C.A. Stan, K. Dieckmann, S. Gupta, M.W. Zwierlein, A. Görlitz, and W. Ketterle, *Phys. Rev. Lett.* **88**, 160401 (2002).

- [5] G. Roati, F. Riboli, G. Modugno, and M. Inguscio, *Phys. Rev. Lett.* **89**, 150403 (2002).
- [6] L. Viverit, C.J. Pethick, and H. Smith, *Phys. Rev. A* **61**, 053605 (2000).
- [7] S.K. Yip, *Phys. Rev. A* **64**, 023609 (2001); H. Pu, W. Zhang, M. Wilkens, and P. Meystre, *Phys. Rev. Lett.* **88**, 070408 (2002).
- [8] M.J. Bijlsma, B.A. Heringa, and H.T.C. Stoof, *Phys. Rev. A* **61**, 053601 (2000); H. Heiselberg, C.J. Pethick, H. Smith, and L. Viverit, *Phys. Rev. Lett.* **85**, 2418 (2000); L. Viverit, *Phys. Rev. A* **66**, 023605 (2002).
- [9] A.P. Albus, S.A. Gardiner, F. Illuminati, and M. Wilkens, *Phys. Rev. A* **65**, 053607 (2002).
- [10] L. Viverit and S. Giorgini, *Phys. Rev. A* **66**, 063604 (2002).
- [11] K. Mølmer, *Phys. Rev. Lett.* **80**, 1804 (1998); M. Amoruso, A. Minguzzi, S. Stringari, M.P. Tosi, and L. Vichi, *Eur. Phys. J. D* **4**, 261 (1998); T. Miyakawa, K. Oda, T. Suzuki, and H. Yabu, *J. Phys. Soc. Jpn.* **69**, 2779 (2000).
- [12] N. Nygaard and K. Mølmer, *Phys. Rev. A* **59**, 2974 (1999); R. Roth and H. Feldmeier, *ibid.* **65**, 021603 (2002).
- [13] A.P. Albus, S. Giorgini, F. Illuminati, and L. Viverit, *J. Phys. B* **35**, L511 (2002).
- [14] R.M. Dreizler and E.K.U. Gross, *Density Functional Theory* (Springer-Verlag, Berlin, 1990).
- [15] S. Beliaev, *Zh. Eksp. Teor. Fiz.* **34**, 433 (1958) [*Sov. Phys. JETP* **7**, 299 (1958)].
- [16] R. Roth, *Phys. Rev. A* **66**, 013614 (2002).
- [17] G. Modugno, G. Roati, F. Riboli, F. Ferlaino, R.J. Brecha, and M. Inguscio, *Science* **297**, 2240 (2002).
- [18] M. Modugno (private communication).